Structural Evaluation of the Second Oldest Glued-Laminated Structure in the United States

Douglas R. Rammer
Engineering Properties of Wood, Wood based Materials and Structures, US Forest Service Forest Products Laboratory, Madison WI, USA drammer@fs.fed.us

Jorge de Melo Moura
Department of Architecture and Urbanization, Universidade Estadual de Londrina, Londrina, Paraná'
Brazil jordan@uel.br

Abstract

The second glued-laminated structure built in the United States was constructed at the USDA Forest Products Laboratory (FPL) in 1934 to demonstrate the performance of wooden arch buildings. After decades of use the structure was decommissioned in 2010. Shortly after construction, researchers structurally evaluated the glued-laminated arch structure for uniform loading on the center arch. This structural system evaluation was added to the existing laboratory work on glued-laminated arches to develop the foundation on which the current glued-laminated arch design criteria is based. After decommisioning, recovered arches were tested in the laboratory to evaluate the loss of structural performance. Loss of structural performance was evaluated by comparing original and current deformation. Based on a preliminary visual and structural assessment, the degradation of structural performance was minimal in the arches, except for one arch that was exposed to a significant amount of water resulting from fighting a building fire.

Keywords: Glued-laminated, arch, historical, structural evaluation, ultrasound

Introduction

General information

In the 1930's the USDA Forest Products Laboratory was engaged in a research program to develop glued-laminated wood beams (Wilson and Cottingham 1952) and arches (Wilson 1939). A seminal project for the glued-laminated research was the construction of an arch building on FPL's campus in winter of 1934 (Figure 1). This building was 13.7 m wide by 48.8 m long and consisted of nine arch lines spaced 4.8 m apart. The base to crown height was 5.7m. Three different arch configurations were utilized. The five central arches were glued-laminated arches with a rectangular cross section having a constant width but a varying depth that was greatest at the knee, near the roof and wall junction, and least at the foundation and roof peak. Adjacent to each span is a wooden arch of double "I" section composed of plywood webs and glued-laminated flanges with a constant width and varying depth, similar to the glued laminated arches. End spans were built with heavy timber trusses connected with shear plate connectors. Spanning between the arches were stress-skin panels consisting of top and bottom plywood panel, glued and nailed to nominal 38 by 140 mm solid sawn lumber. This stiff box configuration assists in spreading forces to adjacent arches.

After decades of use, this structure was deconstructed in the fall of 2010 (Figure 3). Since these arches represent the first generation of both construction adhesives and glued-laminated development, the durability of these arches was evaluated. As part of the overall nondestructive research program, the individual arches were loaded to determine the extent of structural degradation over the past 75 years.

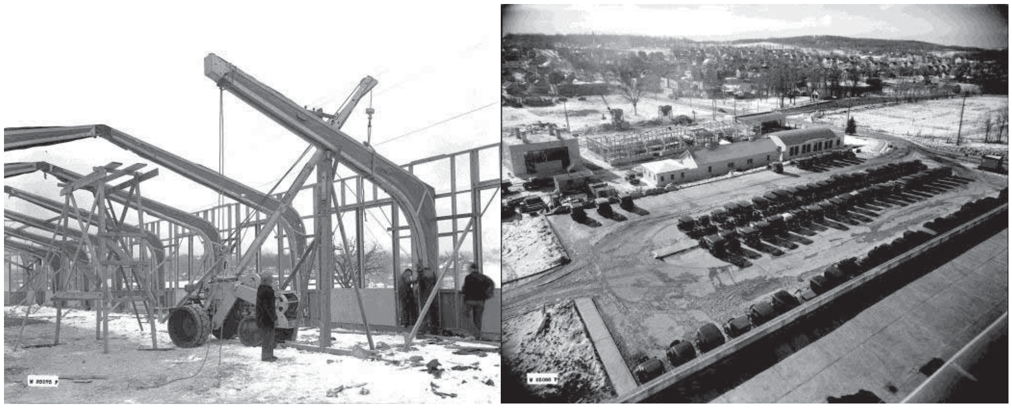

Figure 1—Construction of the USDA Forest Products glued-laminated arch building in the winter of 1934

Figure 2—Deconstruction of FPL's glued-laminated arch building.

Initial Arch Performance

In the fall of 1935, after erection of the structure, the glued-laminated arch structure was incrementally loaded to 140kN with sand bags that were placed uniformly and centered over the full arch span. The load is equivalent to a 295 kN/m^2 on the tributary roof area to one arch and 42% higher than the assumed design live load. Both the immediate and sustained deformations were measured for approximately 224 days between September 1935 and May 1936. Deformations were measured on the loaded arch at the peak and quarter points, while only the peak deformations were measured for the two adjacent arches. Based on these measurements, it was determined that some of the applied uniform load was distributed to the adjacent arches by the stressed-skin panels. Data from this structural evaluation was used to establish both the short term and long-term test procedures used in this study and validated the structural models.

Experimental Procedures

Load Configuration

As stated previously, shortly after the arched structure was constructed, a uniformly distributed load was applied to the center arch line of the structure. For comparison testing of a single arch under a similar loading configuration, this load distribution affect must be accounted for. Application of a uniformly distributed load is troublesome and such loading is typically approximated by a series of concentrated load points.

To conduct experiments on a single half arch in this study, the amount of load redistributed in the original building to adjacent arches was determined. Additional work was needed to determine the location and number of concentrated loads to simulate a uniform loading on the arch arm. This was accomplished through structural analysis of both the original building and a single half arch using MASTAN2 (2006).

Figure 3—Loading of FPL glued laminated arch building and measurement techniques for live loading of building.

For the model of the complete building, each arch was sub-divided into 32 beam elements, each with its cross sectional area and moment of inertia equivalent to those of the mid-span element properties. The upper and lower arch connections were assumed to be hinges, with the base connection having translation restraint. A uniform load, equivalent to the total weight of the sand bags, was applied along the length of the arch arm. The roof system of the arched building consisted of glued plywood and solid sawn stress-skin panels that span the tops of the arches. The lower plywood panel was attached to the arch with six-penny nails spaced every 140 mm. These stress skin members were represented as beams spaced every 1.2 m with section properties using an effective width according to EC5 procedures (Porteous and Kermani 2007). Since the panels were discontinuous over the arch and nails were used to connect the panels to the arch, semi-rigid connections were assumed at the end of the stress-skin beam elements. Effective connection stiffness was adjusted until the model and measured crown deformation of the loaded and adjacent arch along with the ¼ point deformation of the loaded arch were visually matched. Based on the analysis, instead of applying the original 140kN loading to the single full span arch, the laboratory loading was reduced to 106kN to account for the load distributional effects of the roof.

Similarly, a single half arch model was created to determine the number and location of concentrated loads to approximate a uniformly distributed load applied to the arch arm. A linear elastic structural analysis was performed of a single arch that had been sub-divided into 52 beam elements with variations in cross sectional properties. This iterative process continued until the difference between the displacements and moments of the different concentrated and uniform loading conditions were visually minimized. Figure 4 shows the arch deformation for both the series of concentrated loads and the uniformly distributed load conditions, which justifies the approach.

The original loading was uniform across the entire width of the building resulting in peak displacements that were only vertical and rotational. Due to the symmetry of the original testing, only half an arched span was loaded in the laboratory. The peak connection was simulated by welding the original connection plates to a stiff plate that ran on a linear bearing system. This linear bearing facilitated the vertical movement of the arch peak and the connection plates allowed for rotation of the arch end.

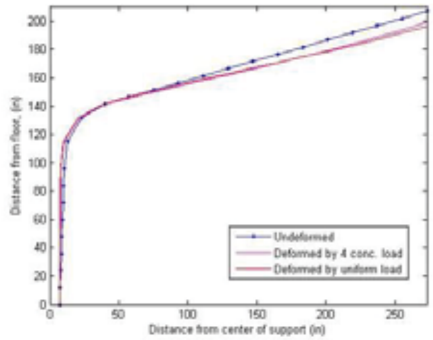

Figure 4—Loading on FPL glued-laminated arch building and measurement techniques for live loading of building.

Loading Protocol

Load was applied to the arch using two 245-kN MTS actuators in tandem under load control until the maximum load was reached. Loads were applied in the following four cycle pattern highlighted in Table 1 with no pauses at the transitions between cycles. For arches 3 and 10, the cycle 3 sustained loading times were extended to 138 and 168 hours, respectively. Figure 5 shows the images of the test setup to achieve the 4-point concentrated load condition.

Table 1—General Loading Protocol for Arches

Cycle	Loading	Sustained	Unloading
1	5 min	10 min	5 min
2	5 min	10 min	5 min
3	5 min	72+ hours	5 min
4	5 min	10 min	5 min

Figure 5— Testing setup of one half of single arch with a four-point loading configuration.

Measurements

Both load and deformation were continually recorded for the duration of the tests, at variable rates. During the loading and unloading of the arches readings were every second, while during the sustained load readings were taken at longer intervals, but not in excess of 30 seconds. Vertical deformations were measured at all quarter points and one horizontal deformation of the arch leg was measured 3.3 m above the support.

Experimental Response

Short Term Loading

Arches were to be loaded with 2 short-term cycles, followed by a sustained load, and finished with one more cycle of short term loading. A typical response to the short term loading cycles are shown in Figure 6a. Note the initial cycle had the greatest deformation response due to the seating of the arch while subsequent short term loadings, cycle 2 and cycle 3 showed nearly identical behavior. Cycle 3short team loading indicated no structural stiffness degrade due to sustained loading just prior. Only arch 5 showed abnormal behavior and only one short term loading was conducted,

Figure 6b. After loading, an inspection revealed that the base of the arch leg had considerable delamination and decay which caused excessive compressive deformation at the base connection. In 1993, the building experienced a fire event. In the course of fighting the fire significant amounts of water pooled at the base of this arch and likely caused the end delamination since the adhesives were not moisture resistant.

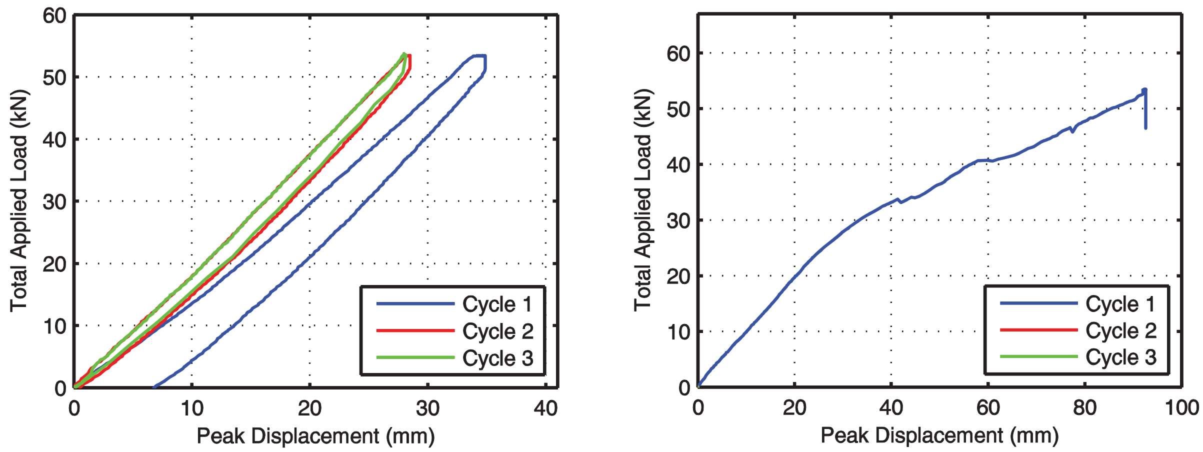

Figure 6— Short term load response for (a) Arch 3 and (b) Arch 5.

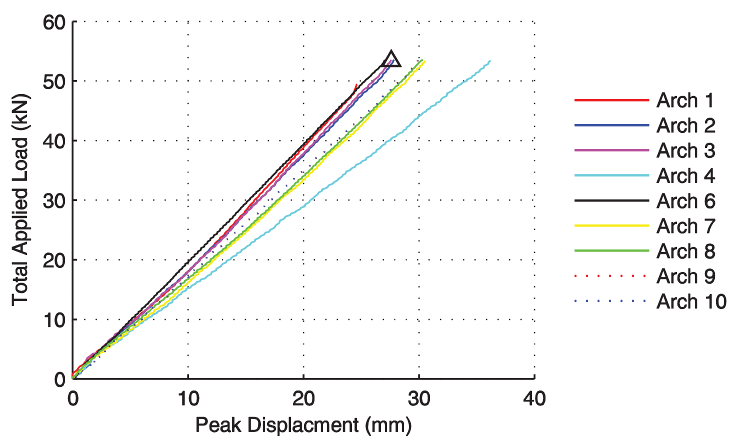

Figure 7— Third cycle, short term, load response for all arches, except 5.

Peak deformation versus applied load, for the third cycle of loading, is plotted in Figure 7 for all arches. Figure 7 indicates all of the arches show a linear response with load, but three distinct observations can be made: 1) arches 1 thru 3 and 6 are grouped together and showed the highest stiffness, 2) arches 8 thru 10 are grouped together at a different and slightly lower stiffness response, and 3) arch 4 stands alone with the lowest linear response. While no reasonable explanation was identified for these groupings, we believe Arches 1 thru 3 and 6 most closely represent the original structure due to the high stiffness, and therefore, are the ideal reference data points for analytical comparisons.

Long Duration Loading

In addition to the short term loading, at least 72 hours of sustained load was applied to the structure between the second and third loading cycles. This longer-term loading provided insight into the potential increase to deformation by sustained loading. During the original loading condition, peak deformation increased about 15 to 20 percent after the first 60 days of loading, while the rate of deformation decreased. After 60 days, the original deformation rate increased but this rate of change was likely due to drying deformations associated with the heating of the building and periodic winter snow loads. To compare the effect that sustained loading has on deformation for all arches we calculated the ratio of the instantaneous measured deformation to deformation when maximum load was first applied. Figure 8 plots this ratio versus time for all measurement locations, for both 72 and 160 hours load durations. Both graphs reveal that larger measured deformations (Peak, ¾ pt, and midspan) gave similar and consistent ratios over the monitoring period. The change in measured deformation was greatest in the first 24 hours of loading, the deformation rate decreased with continued loading, and the deformation increased over the entire monitoring period by about 10 percent. Figure 9 shows the effect of sustained loading on the peak deformation over 72 hours, for all tested arches. For all the arches, the percent of deformation increase was lower than 15 percent and the rate of deformation change was decreasing. These observations lend credence to the statement that measured building deformation changes in the original structure after 60 days were caused by drying of the glued-laminated arches and periodic snow loads, not the original applied loading.

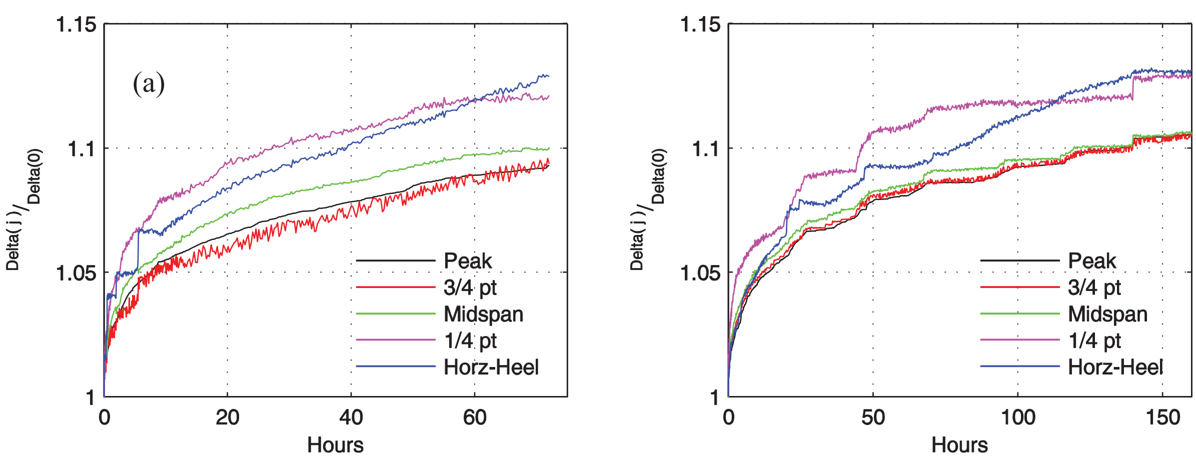

Figure 8— Sustained load deformation response for all measurements for 72 and 160 hours.

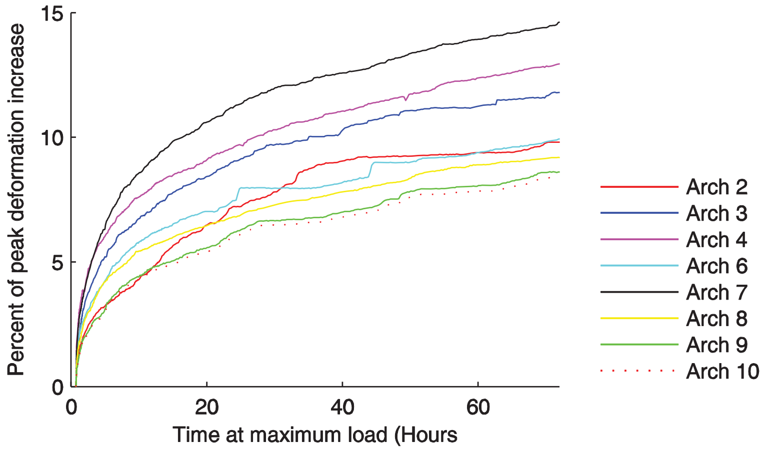

Figure 9— Sustained load response of the peak deformation for all arches, except Arch 5.

Analytical Response

A simple linear elastic model of a single arch was created using MASTAN2, (2006). Though the intention was to simulate uniform loading with four concentrated loads and make a direct comparison, the applied loads were placed at different locations in the laboratory testing. The structural model was reanalyzed for the new loading condition. When the original structure was constructed, two additional arches were manufactured but were tested with a thrust load and from the remains; ASTM D143 property tests were conducted. These material tests estimated a modulus of elasticity of 13.1 GPa. For comparison purposes, the maximum deformation obtained during the laboratory testing of the arches for the final load cycle will be evaluated. Table 2 presents the analytical deformation at the measured deformation locations along with the average, minimum and maximum deformations at maximum load. In general, the model deformations are lower than the average but greater than the minimum measured deflections. Percent difference of the analytical and measured deformations showed similar trends. Figure 7 shows that the model peak deformation (open triangle symbol) and the stiffest group of arches (1,2,3,6) are visually the same.

Table 2—Comparison of Analytical model to experimental measurements

	Deformations (mm)				Percent difference		
Location	Analytical	Average	Min	Max	Average	Min	Max
Peak	27.6	29.3	24.6	36.2	-5.8	12.2	-23.8
¾ Point	20.4	20.1	19.7	27.2	1.5	3.6	-25.0
½ Point	11.7	13.8	12.4	16.8	-15.2	-5.6	-30.4
¼ Point	3.2	5.1	4.7	6.4	-37.3	-31.9	-50.0
Thrust	-7.8	-6.8	-5.7	-9.3	14.7	36.8	-16.1

Connection Issues

The most consistent problem observed after deconstruction of the glued-laminated arch structures was the condition of the crown connection. Figure 10 shows the crown connection consisted of steel side plates attached to the each arch arm with three 25.4-mm bolts in a triangular pattern. Measurements revealed inner bolt end spacing was 2.5d, lower than the minimum 4d required by contemporary design standards. As a result, most of the arch had cracks, splits, or wood plugs emanating from the inner bolts. Figure 10 also shows missing wood material associated with the lower bolt line though this condition was less common. Unlike the middle bolt, sufficient end spacing was provided. There is two possible explanations for this damage. One, after the failure of the inner bolts, the remaining capacity of the connection was insufficient to carry a maximum event load that occurred during the service life to the structure. Two, the connection was damage during deconstruction due to possible out of plane twisting of the arch while it was lowered to the ground (Figure 2). In either case, the damage to the connection had little influence on the vertical loading response of the arches because the splits did not go completely through the cross section. Under a lateral loading scenario, or as the arches reach maximum loading conditions, the connection condition could have a strong influence on behavior.

Figure 10— Peak connection in building and glued-laminated peak with connection plate removed

Conclusions

After 75 years of service, ten glued-laminated arches were recovered for structural evaluation from the deconstruction of the second glued-laminated building built in the United States. Strength loss was assessed by comparing the deformations of single half-arches with a structural model. The structural model was developed and validated using data generated from a 1935 study where the application of a 6-month, in-situ loading of the central span of the original arch structure. Loading of the laboratory half span arches consisted of three cycles of short-term loading and one long-term loading of at least three days. Comparison of the model and experimental deformation reveal that 8 of the 10 arches performed with little or no stiffness loss. One arch had considerable decay and delamination of its leg, and therefore, loading protocols were not completed. Finally, some failures of the glued-laminated edges at the peak connection were observed and attributed to insufficient end spacing of the bolts.

References

Wilson, T.R.C. 1939. The Glued Laminated Wooden Arch. USDA Technical Bulletin No. 691.

Wilson, T.R.C. and Cottingham, W. S. 1952. Tests of glued-laminated wood beams and columns and development of principles of design. Forest Prod. Lab. Rep. R1687.

MASTAN2, version 3.3, developed by Ronald D. Ziemian and William McGuire, 2006

Porteous, J. and Kermani, A. 2007. Structural Timber Design to Eurocode 5. Blackwell Publishing.

United States Department of Agriculture
Forest Service

Forest Products Laboratory

General Technical Report

FPL–GTR–226

Proceedings

18th International Nondestructive Testing and Evaluation of Wood Symposium

Madison, Wisconsin, USA
2013

Abstract

The 18th International Nondestructive Testing and Evaluation of Wood Symposium was hosted by the USDA Forest Service's Forest Products Laboratory (FPL) in Madison, Wisconsin, on September 24–27, 2013. This Symposium was a forum for those involved in nondestructive testing and evaluation (NDT/NDE) of wood and brought together many NDT/NDE users, suppliers, international researchers, representatives from various government agencies, and other groups to share research results, products, and technology for evaluating a wide range of wood products, including standing trees, logs, lumber, and wood structures. Networking among participants encouraged international collaborative efforts and fostered the implementation of NDT/NDE technologies around the world. The technical content of the 18th Symposium is captured in this proceedings.

Keywords: International Nondestructive Testing and Evaluation of Wood Symposium, nondestructive testing, nondestructive evaluation, wood, wood products

September 2013 (Corrected October 2013, pages 716–722)

Ross, Robert J.; Wang, Xiping, eds. 2013. Proceedings: 18th International Nondestructive Testing and Evaluation of Wood Symposium. General Technical Report FPL-GTR-226. Madison, WI: U.S. Department of Agriculture, Forest Service, Forest Products Laboratory. 808 p.

A limited number of free copies of this publication are available to the public from the Forest Products Laboratory, One Gifford Pinchot Drive, Madison, WI 53726–2398. This publication is also available online at www.fpl.fs.fed.us. Laboratory publications are sent to hundreds of libraries in the United States and elsewhere.

The Forest Products Laboratory is maintained in cooperation with the University of Wisconsin.

Contents

Session 1. Industrial Applications of NDT Technologies

Session 2. Nondestructive Evaluation and Hazard Assessment of Urban Trees

Session 3. Nondestructive Evaluation of Standing Timber

Session 4. Nondestructive Evaluation of Logs

Session 5. Condition Assessment of Historic Wood Structures—Experience from Around the Globe

Session 6. Nondestructive Evaluation of Composite Materials—Nanocellulosic Films to Glued Laminated Timber

Session 7. Nondestructive Evaluation of Structural Materials I— New Techniques and Approaches

Session 8. Nondestructive Evaluation of Structural Materials II— Enhancements to Traditional Methods and New Applications

Session 9. Material Characterization I—Acoustic-Based Techniques

Session 10. Material Characterization II—Near Infrared, Neutron Imaging, and Other Techniques

Session 11. Structural Condition Assessment I—NDT Fundamentals and Assessment Methods

Session 12. Structural Condition Assessment II—New Techniques and Field Experiences

Session 13. Poster Session